Carcinogenesis vol.33 no.9 pp.1754–1761, 2012
doi:10.1093/carcin/bgs168
Advance Access Publication July 4, 2012

Accelerated elimination of ultraviolet-induced DNA damage through apoptosis in CDC25A-deficient skin

Jodi Yanagida[1], Brianna Hammiller[1], Jenan Al-Matouq[1], Michaela Behrens[1], Carol S.Trempus[2], Susan K.Repertinger[3] and Laura A.Hansen,[1,*]

[1]Department of Biomedical Sciences, Creighton University School of Medicine, 2500 California Plaza, Omaha, NE 68178, USA, [2]Laboratory of Respiratory Biology, National Institute of Environmental Health Sciences, RTP, NC 27709, USA and [3]Department of Pathology, Creighton University School of Medicine, Omaha, NE 68178, USA

*To whom correspondence should be addressed. Tel: +402 280 4085; Fax: +402 280 2690; Email: LHansen@creighton.edu

Cell division cycle 25A (CDC25A) is a dual-specificity phosphatase that removes inhibitory phosphates from cyclin-dependent kinases, allowing cell-cycle progression. Activation of cell-cycle checkpoints following DNA damage results in the degradation of CDC25A, leading to cell-cycle arrest. Ultraviolet (UV) irradiation, which causes most skin cancer, results in both DNA damage and CDC25A degradation. We hypothesized that ablation of CDC25A in the skin would increase cell-cycle arrest following UV irradiation, allowing for improved repair of DNA damage and decreased tumorigenesis. *Cdc25a$^{fl/fl}$/Krt14-Cre recombinase* mice, with decreased CDC25A in the epithelium of the skin, were generated and exposed to UV. UV-induced DNA damage, in the form of cyclopyrimidine dimers and 8-oxo-deoxyguanosine adducts, was eliminated earlier from CDC25A-deficient epidermis. Surprisingly, loss of CDC25A did not alter epidermal proliferation or cell cycle after UV exposure. However, the UV-induced apoptotic response was prolonged in CDC25A-deficient skin. Double labeling of cleaved caspase-3 and the DNA damage marker γH2A.X revealed many of the apoptotic cells in UV-exposed *Cdc25a* mutant skin had high levels of DNA damage. Induction of skin tumors by UV irradiation of *Cdc25a* mutant and control mice on a skin tumor susceptible to v-*ras^{Ha}* Tg.AC mouse background revealed UV-induced papillomas in *Cdc25a* mutants were significantly smaller than in controls in the first 6 weeks following UV exposure, although there was no difference in tumor multiplicity or incidence. Thus, deletion of *Cdc25a* increased apoptosis and accelerated the elimination of DNA damage following UV but did not substantially alter cell-cycle regulation or tumorigenesis.

Introduction

One of the most serious assaults on the skin is from overexposure to UV in the form of sunlight. UV exposure causes most non-melanoma skin cancer, which is the most common type of cancer in the USA (1). Chronic exposure to UV, including UVB and to a lesser extent UVA, is the major cause of non-melanoma skin cancer because of its DNA-damaging capabilities. Exposure to UVB causes damage to DNA primarily in the form of cyclobutane pyrimidine dimers (CPDs) (2), which causes most UVB-induced mutations (3). Another type of UV-induced DNA damage occurs due to the production of reactive oxygen species. Increasing evidence suggests that the immunosuppressive effects of reactive oxygen species cause conversion of solar keratoses to squamous cell carcinoma (4). A well-known biomarker of oxidative stress is the oxidized guanosine moiety, 8-oxo-deoxyguanosine (8-oxo-dG (5,6)). Point mutations at both the oxidized guanine nucleotide itself and at the base adjacent to the 8-oxo-dG have been found in the *Ras* oncogene in skin and other cancers in response to repair failure (reviewed in ref. 7).

Coordinated regulation of DNA repair and cell-cycle progression is crucial in preventing mutations and cancer. The cell division cycle 25 (CDC25) family of phosphatases, which include CDC25A, CDC25B and CDC25C, regulate progression through the cell cycle and are important for maintaining genomic stability in response to DNA damage (reviewed in ref. 8). Functional overlap in CDC25 family members is probable, since *Cdc25b* and *Cdc25c* null mice develop normally. In contrast, *Cdc25a* null mice are embryonic lethal, consistent with an essential role for CDC25A in cell-cycle progression. These data also suggest that CDC25A may be an important target for cancer therapy (8).

In the normal cell, the removal of the inhibitory phosphates on CDK2 (cyclin-dependent kinase 2) by the protein tyrosine phosphatase CDC25A allows for the activation of CDK2-Cyclin E and CDK2-Cyclin A, enabling advancement into and progression through S-phase (9). In response to UV-induced DNA damage, ataxia telangiectasia and Rad3-related is activated, which leads to degradation of CDC25A (9). Without CDC25A to activate cyclin-CDK complexes, which can result in cell-cycle arrest. Cell-cycle arrest allows time for DNA repair prior to DNA replication, thus preventing mutations (9). Aside from bypassing a mechanism for cell-cycle arrest, overexpression of CDC25A suppresses the cell's response to oxidative DNA damage and stress, which is known to increase cancer risk (10). Further evidence of a role for CDC25A in cancer has been provided by immunohistochemical studies in human cancer. Increased CDC25A protein is found in breast, hepatocellular, ovarian, thyroid, esophageal and colorectal cancers, with its overexpression frequently correlating with increased malignancy and poor prognosis (8). Inhibitors of CDC25 phosphatase activity inhibit growth of transplantable rat hematomas *in vivo* (11), an indication of their promise for clinical use.

Because of the role of the CDC25A phosphatase in DNA damage checkpoints, we hypothesized that deletion of *Cdc25a* in the skin would increase cell-cycle arrest following UV irradiation, allowing for improved repair of DNA damage and decreasing skin tumorigenesis. In order to investigate this hypothesis, the response of mice with a skin-targeted deletion of *Cdc25a* to UV irradiation was examined. This investigation revealed that deletion of *Cdc25a* accelerated elimination of UV-induced DNA damage, increased apoptotic elimination of cells with DNA damage, reduced skin tumor growth at early time points, but surprisingly did not alter cell-cycle regulation or skin tumor multiplicity.

Materials and methods

Animals

Cdc25a$^{fl/fl}$ mice with *loxP* sites inserted flanking exons 1–3 of the *Cdc25a* gene were developed on a C57BL/6 × C3HF1 background as described in (12). *Cdc25a$^{fl/fl}$* mice were crossed with *Krt14* promotor-driven *Cre recombinase* mice on an FVB/N background (The Jackson Laboratory, Bar Harbor, ME) and progeny backcrossed to generate skin-targeted *Cdc25a* knockouts (*Cdc25a$^{fl/fl}$/Cre^{+}*) and controls (*Cdc25a$^{fl/fl}$/Cre^{-}*or *Cdc25a$^{wt/wt}$/Cre^{+}*). *v-ras^{Ha}* transgenic Tg.AC mice on an FVB/N background were crossed with the *Cdc25a* mutants to produce Tg.AC^{+} *Cdc25a* mutants (*Cdc25a$^{fl/fl}$/Cre^{+}*/Tg.AC^{+} and *Cdc25a$^{fl/fl}$/Cre^{+}*/Tg.AC^{-}) and controls (*Cdc25a$^{fl/fl}$/Cre^{-}*/Tg.AC^{+} and *Cdc25a$^{fl/fl}$/Cre^{-}*/Tg.AC^{-}). Genotyping was performed by PCR using the following primers: 5′-CAG AGC CTG AAG TCC TGT GAA GG-3′ and 5′-CTG CCT AGT GTA GTT CCT ACA GCG-3′ (*Cdc25a* (12)); 5′-ACC AGC CAG CTA TCA ACT CG-3′ and 5′-TTA CAT TGG TCC AGC CAC C-3′ and 5′-CTA GGC CAC AGA ATT GAA AGA TCT-3′ and 5′-GTA GGT GGA AAT TCT AGC ATC ATC C-3′ (*Krt14-Cre*, the last two primers produce a positive control band in

Abbreviations: 8-oxo-dG, 8-oxo-deoxyguanosine; ATR, ataxia telangiectasia and Rad3-related; BrdU, bromodeoxyuridine; CDC25A, cell division cycle 25A; CDK2, cyclin-dependent kinase 2; CPD, cyclopyrimidine; DAPI, 4′,6-diamidino-2 phenylindole; TBS-T, Tris-buffered saline Tween 20; TUNEL, terminal dUTP nucleotide end-labeling; UV, ultraviolet.

all samples (13)); and 5′-ATT CTG AAG GAA AGT CC-3′and 5′-TGG ACA AAC TAC CTA CAG-3′ (*Tg.AC* (14)).

UV irradiation and tumor measurements

Eight-week-old *Cdc25a* mutant and control Tg.AC$^-$ mice (for short-term experiments) or 20-week-old *Cdc25a* control and mutant Tg.AC$^+$ mice (for the tumor experiment) were sham or UV irradiated once a week over a period of 4 weeks for a cumulative exposure of 4.3 kJ/m^2. *Cdc25a* mutant and control Tg.AC$^-$ mice exposed to 1 kJ/m^2 or sham irradiated were euthanized 18 h later. UV irradiation was generated using Ultraviolet B TL 40W/12 RS bulbs (The Richmond Light Company, Richmond, VA) covered with Kodacel triacetate film to block UVC (Eastman Kodak, Rochester, NY), resulting in approximately 30% UVA and 70% UVB measured using Oriel Goldilux radiometric photodetector probes (Newport Corporation, Irvine, CA). Dorsal hair was clipped the day before UV irradiation using a Wahl clipper (Wahl Clipper Corporation, Sterling, IL) and close shaved with a Braun Series 3 shaver (Proctor and Gamble, Cincinatti, OH) just before exposure. Mice were injected with approximately 0.075 mg per gram body weight bromodeoxyuridine (BrdU) (Sigma-Aldrich, St.Louis, MO) 1 h before euthanasia. Tumor diameter in two dimensions was measured using calipers and tumor size calculated as length times width. All procedures were approved by the Creighton University Institutional Animal Care and Use Committee.

Immunoblotting

Epidermis was separated from the skin using the heat shock method as described in (15). Protein was extracted from tumors or epidermis in lysis buffer containing 10 mM Tris (pH 7.4), 150 mM sodium chloride, 10% glycerol, 1% Triton X-100, 1 mM ethylenediaminetetraacetic acid, 1X Complete Protease Inhibitor Cocktail (Roche, Germany), 1 mM sodium orthovanadate (ICN Biomedicals, Aurora, OH), 1.5 µM ethylene glycol tetraacetic acid (Sigma, St.Louis, MO) and 10 µM sodium fluoride using a tissue homogenizer (Tissue Master 125, Omni International LLC, Bedford, NH). Protein was quantified using Coomassie Brilliant Blue G-250 (Bio-Rad, Hercules, CA). Immunoblotting was performed using standard techniques with antibodies recognizing CDC25A (1:200 Santa Cruz, Santa Cruz, CA), actin (Sigma-Aldrich, St.Louis, MO) or glyceraldehyde 3-phosphate dehydrogenase (GAPDH) (Cell Signaling, Boston, MA). Horseradish peroxidase–conjugated secondary antibodies (Cell Signaling, Beverly, MA), chemiluminescent reagents (Pierce, Rockford, IL) and autoradiography were used to visualize results. Ponceau S staining (Sigma-Aldrich, St.Louis, MO) and actin immunoblotting confirmed the evenness of loading and transfer. Densitometry was performed using ImageLab software (Bio Rad Life Science Research, Rochester, NY).

Immunostaining, TUNEL and morphometric analyses

Hematoxylin and eosin (Sigma-Aldrich, St.Louis, MO) staining was performed using standard techniques. Ethanol-fixed tissue sections were incubated in BrdU (1:3, Becton Dickinson, Franklin Lakes, NJ) or CPD (1:1000, Kamiya Biomedical, Seattle, WA) antibody and formalin-fixed sections were incubated in cleaved caspase-3 (Cell Signaling, Beverly, MA) or phospho-histone H2A.X (Millipore, Billerica, MA) antibody. Sections were then incubated in Alexa-Fluor 488 (Invitrogen, Carlsbad, CA) or biotinylated F(Ab)$_2$ fragment goat antimouse secondary (Jackson ImmunoResearch, West Grove, PA), followed by Texas-Red Streptavidin (Vector Laboratories, Burlingame, CA) and 4′,6-diamidino-2-phenylindole (DAPI) in mounting media (Molecular Probes, Invitrogen, Carlsbad, CA). Terminal transferase dUTP nick-end labeling (TUNEL) (Promega, Madison, WI) was performed following the manufacturer's protocol. Immunohistochemistry for CDC25A was performed using anti-CDC25A antibody (Santa Cruz, CA), horseradish peroxidase–conjugated secondary antibody (Vector Labs, Burlingame, CA), diaminobenzidine substrate (Sigma Chemical Corp.) and hematoxylin counterstain (Sigma Chemical Corp). For some experiments, cleaved caspase-3 and γH2A.X immunofluorescence were performed as described above and results photographed. Coverslips were removed and slides were washed overnight with agitation with several changes of phosphate-buffered saline and incubated in stripping solution containing 200 µM glycine and 3.5 µM sodium dodecyl sulfate (Fisher Scientific), before immunohistochemistry for CDC25A. Controls for the immunostaining and TUNEL included replacing enzyme with buffer for TUNEL and replacing primary antibody with buffer for immunostaining. BrdU- and TUNEL-positive cells were quantified by counting positively stained cells and the DAPI-positive basal cells in each section using a ×20 objective with the investigator blinded as to the identity of the sample.

Flow cytometric analysis

Cell-cycle analysis was performed using flow cytometry of 50 µm sections from formalin-fixed paraffin-embedded blocks as described in (16). The sections were deparaffinized, rehydrated, digested in 0.05% pepsin (Sigma, St.Louis, MO) in phosphate-buffered saline with pH 1.5 and then incubated in Tris Buffered Saline (pH 7.6), Ribonuclease-A, propidium iodide and IGEPAL CA-630 (Sigma, St.Louis, MO (17)) before analysis using a FACSCalibur flow cytometer (Becton Dickinson, Franklin Lakes, NJ) and CellQuest analysis (BD Biosciences, San Jose, CA).

Southwestern assays

Epidermis was collected by liquid nitrogen scraping of flash-frozen skin as in (18). DNA was extracted from the epidermis by incubating in buffer containing 200 µg/ml Proteinase K and 100 mM NaCl in 10% SDS, 50 mM EDTA and 100 mM Tris (pH 8.0). DNA was precipitated in 4.21 M NaCl, 0.63 M KCl and 10 mM Tris (pH 8.0) with two volumes 100% ethanol. DNA was resuspended in 0.4 mM NaOH and 0.1 mM EDTA (Sigma, St.Louis, MO), heated to 95°C and neutralized with 2 M ammonium acetate. DNA was blotted onto a nitrocellulose membrane, dried, blocked in 5% bovine serum albumin in Tris-buffered saline with 0.1% Tween-20 (TBS-T), incubated in primary antibody (Anti-8-oxo-dG, 1:500, Japan Institute for Control on Aging, Shizuoka, Japan or Anti-Thymine Dimer, 1:500, Kamiya Biomedical Company, Seattle, WA), washed in TBS-T, incubated in horse antimouse IgG horseradish peroxidase–linked secondary (1:10 000, Cell Signaling Technologies, Beverly, MA) in 5% bovine serum albumin /TBS-T. Blots were washed in TBS-T and signal was detected by incubation with LumiGLO chemiluminescent Reagent (1:1, Cell Signaling Technologies) using a BioRad Chemidoc XRS+ (Bio Rad Life Science Research, Hercules, CA) or by exposure of Kodak BioMax Film (Carestream Health, Rochester, NY). Densitometry was performed using ImageLab software (Bio Rad Life Science Research).

Statistical analyses

A Student's two-tailed *t*-test or two-way analysis of variance (ANOVA) were used to determine statistical significance. $P \leq 0.05$ was considered to be significant.

Results

Deletion of Cdc25a-accelerated elimination of DNA damage from UV-exposed skin

To test our hypothesis that deficiency of CDC25A allows for more efficient repair of DNA damage following UV irradiation, skin-targeted *Cdc25a* mutant mice were developed by breeding mice homozygous for loxP sites inserted flanking exons 1 through 3 of *Cdc25a* (*Cdc25a$^{fl/fl}$*) with *Krt14* promoter-driven *Cre recombinase* (*Cre$^+$*) mice. *Cdc25a* mutant mice (*Cdc25a$^{fl/fl}$/Cre$^+$*) were healthy and viable, with no obvious phenotype. Immunoblotting revealed reduced CDC25A protein in mutant epidermis (Figure 1A). CDC25A protein was localized primarily in the epidermis of control mice, with both nuclear and cytoplasmic staining apparent (Figure 1B), as has been previously described in other tissues (19). *Cdc25a* mutant skin, in contrast, had patches of CDC25A positivity intermixed with CDC25A negative cells in the epidermis (Figure 1B). Groups of *Cdc25a* control and mutant mice were exposed to UV once a week for 4 weeks and DNA damage in the form of cyclopyrimidine dimers was detected using a CPD-specific antibody in immunofluorescence assays. CPDs were not detected in sham-irradiated skin (Figure 2A). After 12 h

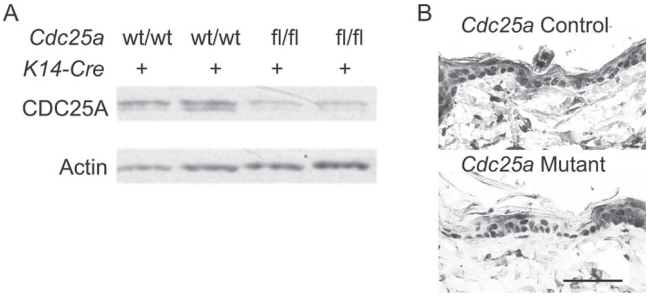

Fig. 1. Decreased CDC25A protein in *Cdc25a* mutant epidermis. (**A**) Epidermis from *Cdc25a* mutant and littermate control mice was immunoblotted as indicated. Each lane is protein from a separate mouse. (**B**) Immunohistochemistry for CDC25A (brown) in untreated *Cdc25a* mutant and littermate control mice with a hematoxylin counterstain (blue). Scale bar indicates 50 µm.

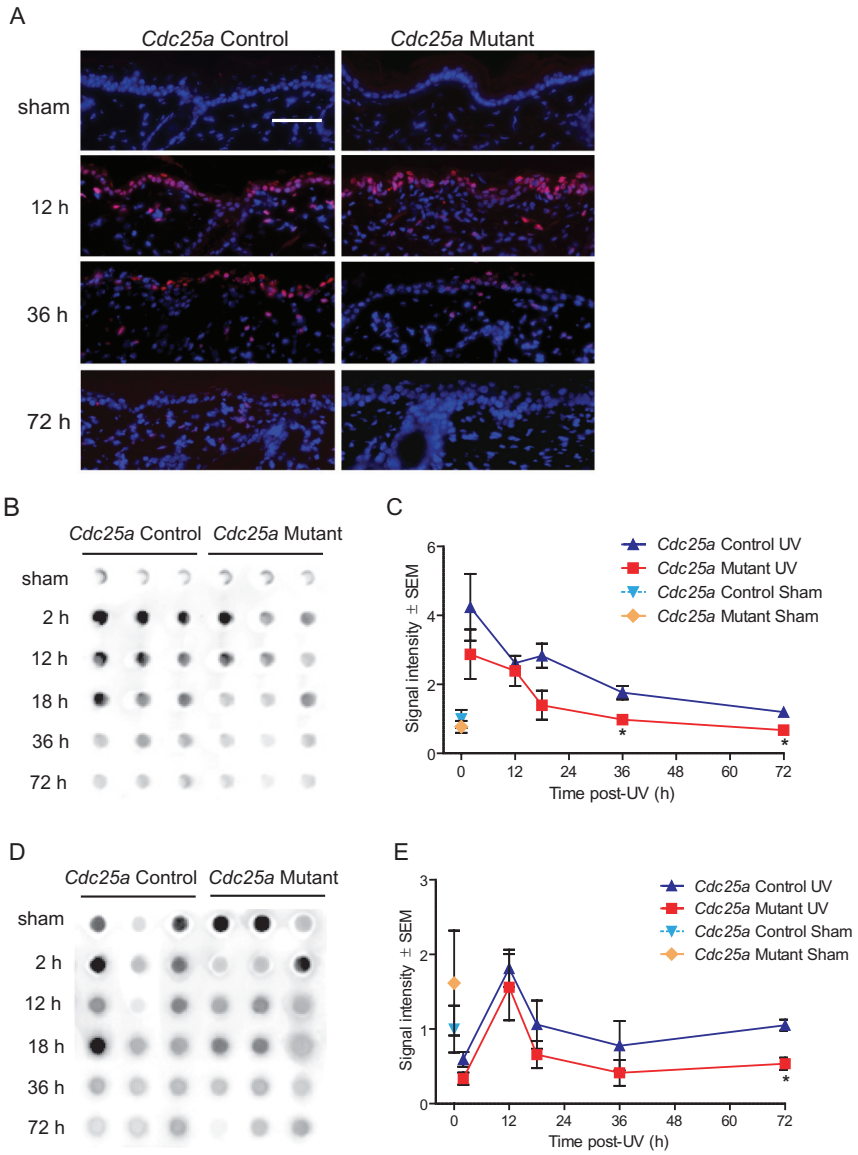

Fig. 2. Improved elimination of UV-induced DNA damage in CDC25A-deficient epidermis. (**A–D**) Groups of 8-week-old *Cdc25a* mutant and littermate control mice were exposed four times for a cumulative dose of 4.3 kJ/m^2 UVA/B or were sham irradiated and euthanized at the indicated time points following the last exposure ($N \geq 3$ mice). Representative images for immunofluorescence for CPD shown, with CPD in red and DAPI in blue (**A**). Southwestern blots using CPD (**B**) or 8-oxo-dG (**D**) antibodies are shown, where each spot is DNA from a separate mouse. DNA (0.25 µg) from each mouse was blotted in duplicate on each membrane (not shown). Quantification of multiple Southwestern assays for CPD (**C**) or 8-oxo-dG (**E**) was averaged. *Indicates a significant difference compared to the corresponding UV-exposed control group using ANOVA, where $P \leq 0.05$. Scale bar indicates 60 µm.

of UV irradiation, CPDs were detected in the basal and suprabasal keratinocytes of the epidermis, as well as fibroblasts of the superficial dermis (Figure 2A). In order to quantify CPDs, Southwestern assays were performed using isolated epidermis, revealing levels of cyclopyrimidine dimers that peaked 2 h following UV irradiation in both mutant and control mice (Figure 2B and 2C), corresponding to the rapid formation of cyclopyrimidine dimers in both mutant and control mouse skin. Consistent with our hypothesis, mutant *Cdc25a* skin eliminated cyclopyrimidine dimers from the epidermis more rapidly as evidenced by the return to background, sham-irradiated levels by 36 h following UV, whereas controls still had elevated CPDs at 72 h (Figure 2A and 2C).

Another form of DNA damage resulting from the formation of reactive oxygen species in response to UV irradiation is the 8-oxo-dG adduct (6). Southwestern assays were performed using an 8-oxo-dG antibody in order to quantify relative levels of 8-oxo-dG in *Cdc25a* control and mutant epidermis. Surprisingly, sham-irradiated mouse skin had more 8-oxo-dG than at 2 h after UV irradiation for both *Cdc25a* controls and mutants (Figure 2D and 2E). Thereafter, levels peaked at 12 h post-UV before declining. The 8-oxo-dG adducts were removed from *Cdc25a* mutant epidermis earlier than from controls, with significantly less in mutants compared with controls at 72 h following UV (Figure 2E). Consistent with our hypothesis, CPDs and 8-oxo-dG adducts were removed from *Cdc25a* mutant skin more quickly than from controls.

Deletion of Cdc25a did not reduce cutaneous proliferation

In order to determine whether accelerated removal of UV-induced DNA damage upon deletion of *Cdc25a* was due to cell-cycle arrest in *Cdc25a* mutant epidermis, both the cell proliferation and the cell cycle were examined. Quantification of BrdU-positive cells as a measure of cell proliferation revealed no difference in the number of BrdU-positive cells in sham-irradiated *Cdc25a* mutant and control epidermis (Figure 3A and 3B). There was little change in BrdU

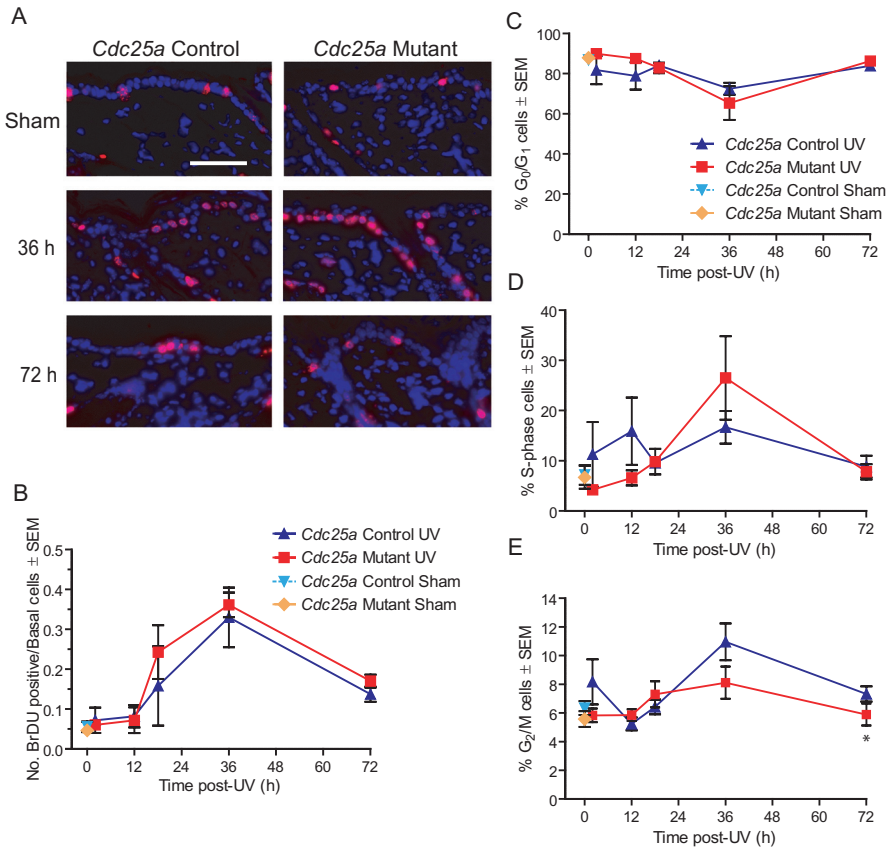

Fig. 3. Unaltered proliferative response to UV irradiation upon deletion of *Cdc25a*. Groups of 8-week-old *Cdc25a* mutant and littermate control mice were exposed four times for a cumulative dose of 4.3 kJ/m^2 UVA/B or were sham irradiated and euthanized at the indicated time points following the last exposure. Representative images for BrdU immunofluorescence (**A**) and quantification of BrdU labeling index (**B**) are shown. Red is BrdU and blue is DAPI (**A**). Bar indicates 60 μm (**A**). DNA content flow cytometry was performed on 50 μm skin sections and the percentage of G_0/G_1 (**C**), S-phase (**D**) and G_2/M cells (**E**) are shown. *Indicates a significant difference when compared with the corresponding UV-exposed control group using two-way ANOVA, where $P \leq 0.05$ (**E**).

labeling after UV irradiation in either genotype until 18 h (Figure 3B). By 18 h following UV irradiation, proliferation began to increase and then peaked at 36 h post-UV irradiation in both genotypes before declining (Figure 3A and 3B). Surprisingly, there was no significant difference in BrdU incorporation between the *Cdc25a* mutants and controls at any time point following UV irradiation (Figure 3A and 3B).

To further examine the effect of CDC25A on the cell cycle, DNA content flow cytometry was performed. Similar to the BrdU incorporation results, the percentage of cells in S-phase increased significantly between 2 h and 36 h post-UV irradiation for *Cdc25a* mutants ($P = 0.01$), with a corresponding decrease in G_0/G_1-phase cells, and then S-phase cells declined (Figure 3C and 3D). Although there were no significant differences in a direct comparison of the genotypes, S-phase cells did not increase significantly between 2 h and 36 h post-UV irradiation in the control genotype ($P = 0.60$). Interestingly, mean G_2/M-phase cells were significantly reduced in UV-exposed *Cdc25a* mutant compared with control mice (Figure 3E). Taken together, these results reveal surprisingly little effect of CDC25A on the cell cycle following UV exposure.

UV-induced apoptosis was prolonged in Cdc25a mutants compared with controls

Given that elimination of DNA damage was improved in the absence of cell-cycle arrest in *Cdc25a* mutant skin, we hypothesized that ablation of *Cdc25a* might increase apoptosis in response to UV irradiation. The number of TUNEL-positive epidermal cells increased in *Cdc25a* controls following UV exposure, peaking at 12 h and then decreasing to near baseline levels by 18 h (Figure 4A, arrowheads, Figure 4B). An increase in TUNEL positivity in the superficial cells of the dermis was also detected after UV irradiation (Figure 4A). Although the numbers of *Cdc25a* mutant TUNEL-positive epidermal cells were similar 12 h after UV exposure, mutant skin had significantly more TUNEL-positive cells at 18 h following UV in comparison with control skin (Figure 4A, arrowheads, Figure 4B). Staining of cleaved caspase-3 positive cells also demonstrated maximal apoptosis in *Cdc25a* control and mutant epidermis 12 h post-UV irradiation (Figure 4C, green nuclei). In addition, increased apoptosis in mutant epidermis compared with control was confirmed at 18 h post-UV irradiation (Figure 4C, green nuclei).

To determine whether increased apoptosis in mutant skin was a mechanism for the elimination of cells with DNA damage, double labeling of cleaved caspase-3, an apoptotic marker, and γH2A.X, a DNA damage marker, was performed. Many cleaved caspase-3 positive cells were also positive for phosphorylated histone γH2A.X (Figure 4C, arrows). Triple labeling for CDC25A, cleaved caspase 3 and γH2A.X revealed some cells lacking CDC25A that were positive for both cleaved caspase-3 and γH2A.X (Figure 4D, arrows). Surprisingly, apoptotic cells were also detected adjacent to, as well as distant from, cells with DNA damage (Figure 4C). Thus, genetic deletion of *Cdc25a* in murine epidermis increased apoptotic death of cells with DNA damage following UV irradiation.

Decreased tumor growth in Cdc25a-deficient mice without altered tumor incidence or tumor multiplicity

In order to examine the influence of CDC25A on UV-induced skin tumorigenesis, *Cdc25a* mutants and controls were crossed with v-*ras*^{Ha} transgenic Tg.AC mice, which were genetically initiated to develop skin papillomas after minimal exposure to UV (20,21). These

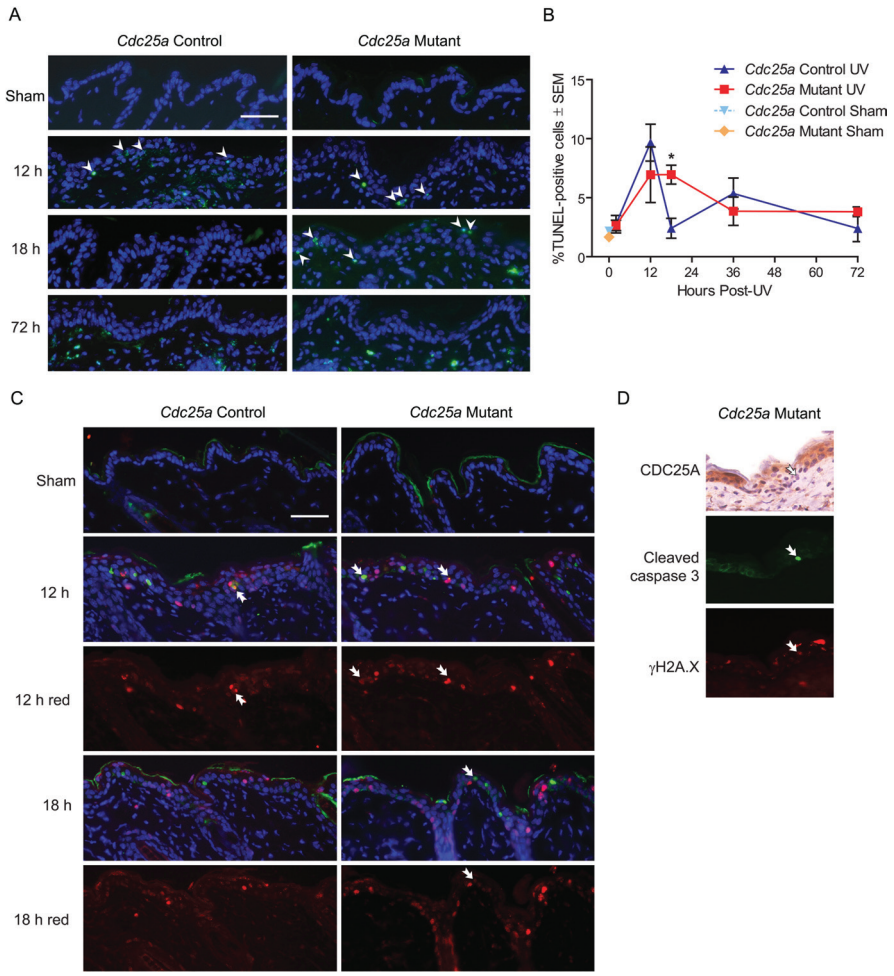

Fig. 4. Increased UV-induced apoptosis of cells with DNA damage in *Cdc25a* mutant epidermis. (**A–D**) Groups of 8-week-old *Cdc25a* mutant and littermate control mice were exposed four times for a cumulative dose of 4.3 kJ/m^2 UVA/B or were sham irradiated and euthanized at the indicated time points following the last exposure. Representative images for TUNEL (**A**) and quantification of TUNEL labeling index in the epidermis (**B**) are shown. Blue is DAPI and green is TUNEL-positive cells (**A**). (**A**) Arrowheads indicate TUNEL-positive epidermal cells and scale bar indicates 60 µm. (**B**) *Indicates a significant difference when compared with the corresponding UV-exposed control group using two-way ANOVA, where $P \leq 0.05$ (B). (**C**) Representative images of double labeling for cleaved caspase-3 (green) as a measure of apoptosis, γH2A.X (red) as a measure of DNA damage, and DAPI (blue) to identify nuclei are shown. Photomicrograph showing red fluorescence only is shown below the multicolor panels at 12 and 18 h for better visualization of γH2A.X immunofluorescence. Arrows indicate cleaved caspase-3- and γH2A.X-double positive cells. Scale bar indicates 60 µm. (D) CDC25A immunohistochemistry (top), cleaved caspase-3 immunofluorescence (middle) and γH2A.X immunofluorescence (bottom) is shown in *Cdc25a* mutant skin 18 h post-UV. The arrow indicates a CDC25A-negative keratinocyte that is positive for caspase-3 (green) and γH2A.X (red).

transgenic mice have markedly increased susceptibility to the development of UV-induced skin tumors, allowing for easy quantification of tumors in response to UV. Mutations in c-*ras*^{Ha} occur in up to 46% of human non-melanoma skin cancers (22–25), supporting the relevance of the Tg.AC model for skin cancer research. Tumors were first observed in UV-exposed *Cdc25a* control mice at 3 weeks after the start of UV irradiation and at 4 weeks in the mutants (Figure 5A). By 5 weeks, Tg.AC$^+$/*Cdc25a* mutants had an average of 1 tumor per mouse and controls had about 2.5 tumors per mouse. Tumor number in the controls peaked at 6 weeks with a mean of 4.3 tumors per mouse. In the mutants, tumor number peaked at 7 weeks with nearly 4 tumors per mouse (Figure 5A). Tumor multiplicity decreased after this primarily due to euthanasia of moribund mice or of mice with a heavy tumor burden. There were no statistical differences in tumor multiplicity or tumor incidence between genotypes at any time point (Figure 5A-B). Between 4 and 6 weeks following the start of the experiment, *Cdc25a* mutants had significantly smaller tumors as compared with controls (Figure 5C). However, between 7 and 9 weeks post-UV irradiation, a large decrease in the mean tumor area for the *Cdc25a* control group upon euthanasia of one mouse with a high tumor burden eliminated this difference (Figure 5C). At later time points, tumor areas were similar in the two genotypes, as some mice were euthanized for health reasons, and tumor area did not significantly differ between the two groups for the duration of the experiment. Histopathological characterization revealed that most lesions were well-circumscribed, exophytic tumors with marked papillomatosis, acanthosis and variable hyperkeratosis (Supplementary Figure 1 is available at *Carcinogenesis* Online). Mitotic activity was minimal and no epithelial atypia or invasion was noted. A single squamous cell carcinoma *in situ* was identified in each of the UV-exposed *Cdc25a* mutant and control groups.

To determine whether decreased CDC25A was maintained in the tumors, immunoblotting for CDC25A was performed with tumors obtained within the last 2 weeks of the experiment. As shown in Figure 5D, CDC25A was not decreased in the *Cdc25a* mutant tumors as it was in *Cdc25a* mutant skin (Figure 1A and 1B). Real-time RT–PCR demonstrated similar *Cdc25a* transcripts in tumors from *Cdc25a* mutant and control mice (data not shown). Because stromal

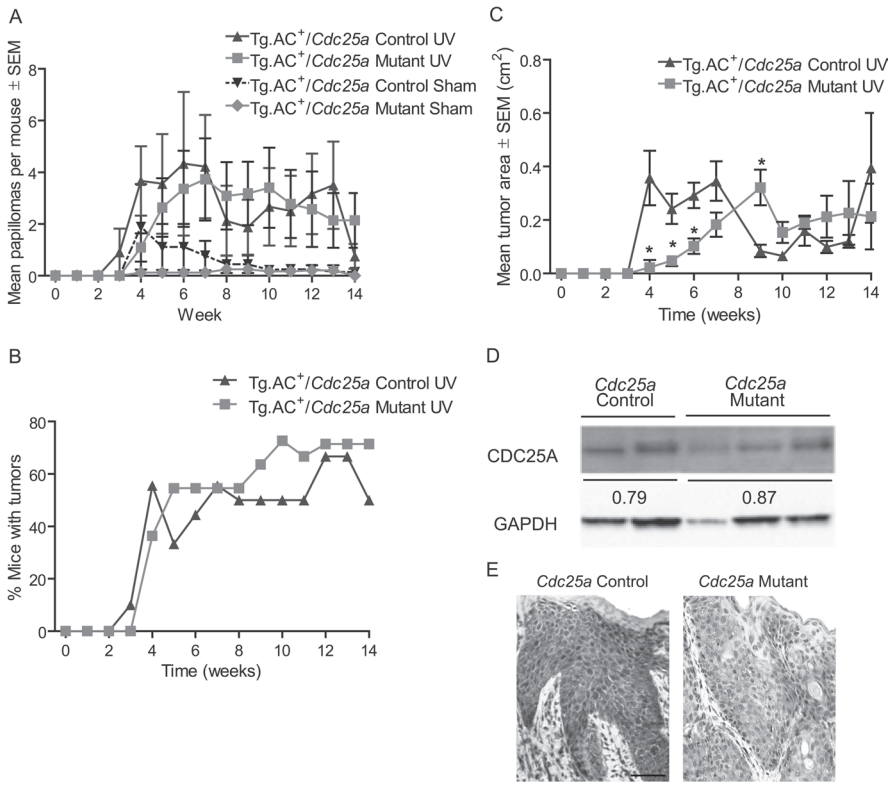

Fig. 5. Smaller tumors in UV-exposed *Cdc25a* mutant skin but no difference in tumor incidence or multiplicity. (**A–F**) Groups of 20-week-old *Cdc25a* mutant and littermate control mice were exposed four times for a cumulative dose of 4.3 kJ/m^2 UVA/B or were sham irradiated and tumor development monitored (N = 10 mice). Tumor multiplicity (**A**), tumor incidence (**B**) and mean tumor area (**C**) are shown. *Indicates a significant difference when compared to the corresponding *Cdc25a* control group. (**D**) Immunoblotting of papillomas using the indicated antibodies. Numbers under the panel indicate the mean for densitometry after normalization to GAPDH. Each lane is protein from a separate tumor. (**E**) Immunohistochemistry for CDC25A in *Cdc25a* mutant and control papillomas. Brown is CDC25A immunostaining and blue is hematoxylin counterstain. Scale bar indicates 50 μm.

CDC25A could mask decreased CDC25A protein or transcripts in the mutants in these experiments, CDC25A localization was also examined. Although CDC25A immunostaining of mutant skin revealed patches of cells with strong CDC25A staining next to regions lacking CDC25A immunopositivity (Figure 1B), CDC25A was detected uniformly in mutant tumor epithelium although with fainter signal than in control tumor epithelium (Figure 5E). CDC25B and CDC25C were also detected in control and mutant tumors but were not increased in mutants compared with controls, indicating no compensatory upregulation of other family members in the mutant tumors (data not shown). Real-time RT–PCR for *Cdc25b* and *Cdc25c* also did not reveal any compensatory increase in *Cdc25a* family member expression that may have been detected non-specifically by the CDC25A antibody (data not shown). Taken together, these experiments suggest a negative selection pressure for cells lacking CDC25A during UV-induced skin tumorigenesis.

Discussion

Although CDC25A is overexpressed in a number of internal cancers including breast, colorectal and esophageal cancer and associated with a poor prognosis (8), little is known about the role of CDC25A in skin carcinogenesis. The CDC25A phosphatase plays an important role in cell-cycle regulation through its deactivation of cyclin-dependent kinases. Previous experiments in our laboratory have shown that Erbb2 activation in response to UV irradiation maintains CDC25A levels, allowing for cell-cycle progression (16). Inhibition of Erbb2 leads to decreased CDC25A, increased S-phase arrest and reduced skin tumorigenesis following UV irradiation. For these reasons, the role of CDC25A in UV-induced skin carcinogenesis and the response of skin to UV were investigated.

In order to investigate the role of CDC25A in non-melanoma skin tumorigenesis, a skin-targeted *Cdc25a* mutant mouse was created by utilizing a *Krt14* promoter-driven *Cre recombinase* gene. *Krt14* is expressed in the basal layer of the epidermis by embryonic day 14 (26), before development of hair follicles as outgrowths of the epidermis or differentiation of the basal layer into multilayered squamous epidermis (27–29). We expected that *Cdc25a* would be targeted to keratinocytes of the skin, both in the epidermis and in the hair follicles. Our results are consistent with incomplete excision of the floxed allele in the cre/loxP system (30), as our immunoblotting and immunostaining results revealed some CDC25A protein in *Cdc25a*$^{fl/fl}$/*Cre*$^+$ epidermis. Moreover, CDC25A protein was detected uniformly in mutant tumor epithelium, indicating a selection bias for *Cdc25a* intact cells during tumorigenesis.

The skin-targeted *Cdc25a* knockout model was used to investigate the hypothesis that deletion of *Cdc25a* increases cell-cycle arrest following UV irradiation, resulting in improved repair of DNA damage and decreased skin tumorigenesis. Consistent with our hypothesis, the UV signature CPD lesion and the oxidized base 8-oxo-dG were removed from the epidermis more rapidly in UV-exposed *Cdc25a* mutants compared with UV-exposed controls. Removal of DNA damage may have been due to accelerated repair, altered cell-cycle kinetics or increased apoptosis of cells with DNA damage. Although nucleotide excision repair can be used for oxidative damage (reviewed in ref. 31), CPDs and 8-oxo-dGs would normally be repaired through distinct mechanisms, nucleotide excision repair for CPDs and base excision repair for 8-oxo-dG as reviewed in ref. 5. Thus, our results

suggest CDC25A modulation of cell-cycle arrest or cell death facilitates elimination of the damage rather than a direct effect on DNA damage repair pathways. Consequently, we anticipated that ablation of *Cdc25a* would increase S-phase arrest due to its established role in cell-cycle regulation. Surprisingly, however, deletion of *Cdc25a* had minimal effects on the cell cycle after UV irradiation. In addition to the analyses of proliferation following several exposures to UV, a similar analysis of BrdU incorporation was performed using *Cdc25a* mutant and control skin 18 h after 1 kJ/m^2 UV irradiation, revealing no significant differences between genotypes using a Student's *t*-test ($P = 0.29$).

In the absence of cell-cycle changes to account for improved elimination of UV-induced DNA damage, apoptotic cell death was examined. In control mice, UV-induced apoptosis peaked at 12 h and then declined precipitously by 18 h. In the mutant skin, in contrast, apoptosis increased at 12 h and was maintained at that elevated level until 18 h, as observed both through TUNEL and cleaved caspase-3 immunofluorescence. Because many cleaved caspase-3 positive cells were also positive for phosphorylated histone H2A.X, and some of these were lacking CDC25A, the elevated apoptosis would result in the elimination of cells with DNA damage. Thus, accelerated removal of CPDs and 8-oxo-dG adducts in *Cdc25a* mutants was likely due to increased apoptosis of damaged cells. A role for CDC25A in suppression of apoptotic cell death has previously been documented by Zou, et al. (10) who found that CDC25A interacts directly with and inhibits apoptosis signal-regulating kinase 1, which is activated in response to reactive oxygen species and regulates multiple proteins involved in the cellular stress-response pathway leading to apoptosis. Thus, CDC25A may inhibit the apoptotic response to oxidative stress. In our hands, CDC25A appeared to limit the apoptotic response to UV, although the mechanism for this effect awaits further investigation.

The influence of CDC25A on UV-induced tumor development was evaluated in *v-ras^{Ha}* Tg.AC mice, a genetically initiated model that rapidly and uniformly develops skin tumors in response to carcinogens such as UV irradiation. The mutant transgene in this model is relevant to human skin carcinogenesis, because up to 46% of human cutaneous squamous-cell carcinomas have *Ras* mutations (22–25). There was no difference in tumor number or incidence between *Cdc25a* mutant and control genotypes. However, *Cdc25a* mutant mice had slower growing skin tumors, as tumor area in the mutant group was statistically less than *Cdc25a* controls in the first 6 weeks of the experiment. This difference disappeared at later time points, as some mice with high tumor burdens were euthanized for humane reasons. Thus, in these experiments, deletion of *Cdc25a* reduced tumor growth only early on but did not affect tumor number. The increased apoptosis in *Cdc25a* mutant keratinocytes following UV exposure may have resulted in decreased growth of tumors at early time points. Because the *Cdc25a* deletion is inefficient in this model, an increase in cell death in *Cdc25a* mutant cells may have led to the overgrowth of CDC25A-expressing cells over time. This could result in the differences between *Cdc25a* mutants and controls disappearing at later time points, consistent with our data. The improved elimination of DNA damage in *Cdc25a* mutant mice predicted decreased tumorigenesis in the mutants. The lack of decrease in tumor number upon deletion of *Cdc25a* may be a consequence of the Tg.AC model used, because in this model tumor development correlates strongly with proliferative and hyperplastic responses (32). Because only four exposures to UV are adequate to promote tumors in this model, UV-induced DNA damage may have had less influence on tumorigenesis than UV-induced cell proliferation. Alternatives to the Tg.AC model, such as UV irradiation of *Cdc25a* mutant mice on a hairless SKH-1 background, might reveal a more pronounced effect of CDC25A. Alternatively, the lack of deletion of *Cdc25a* in many epidermal cells (Figure 1B) may have allowed for the development of CDC25A-expressing tumors in the mutant mice, a hypothesis consistent with our immunoblotting, immunostaining and real-time RT–PCR results using mutant and control tumors. It is also possible that CDC25B and CDC25C could compensate for the loss of CDC25A in the skin, as has been shown previously in adult mice (12). However, real-time RT–PCR and immunostaining did not show increased CDC25B or CDC25C in mutant tumors (data not shown).

To summarize, decreased levels of CDC25A in UV-irradiated skin resulted in accelerated removal of DNA damage in the epidermis and increased apoptotic cell death, which were accompanied by decreased tumor growth but no change in tumor number. Inhibitors of CDC25A have been developed such as the vitamin K dual-specificity phosphatase inhibitor Cpd5 and the CDC25A-specific phenyl maleimide 20 (PM-20, (33,34)). PM-20 reduces the tumor burden in rat liver cancer *in vivo* (34). Thus, in other organs, CDC25A has been shown to be a promising target for anticancer therapy. The data presented here, however, document improved elimination of DNA damage, increased UV-induced apoptosis and delayed tumor growth in *Cdc25a* mutant skin, but no differences in the number of UV-induced skin tumors in *Cdc25a* mutant mice. Further experiments are required to fully evaluate the influence of CDC25A and its potential importance as a therapeutic target in skin cancer.

Supplementary material

Supplementary Figure 1 can be found at http://carcin.oxfordjournals.org/

Funding

National Institutes of Health (1RO1ES015585) and the State of Nebraska Cancer and Smoking-Related Diseases Research Program. This investigation was conducted in a facility constructed with support from Research Facilities Improvement Program (1CO6RR17417-01, G20RR024001) from the National Center for Research Resources, National Institutes of Health. This work was conducted in part in the Intramural Research Division of the National Institutes of Health/National Institute of Environmental Health Sciences. The content is solely the responsibility of the authors and does not necessarily represent the official views of the National Center for Research Resources or the National Institutes of Health.

Acknowledgements

We thank Dr. Helen Piwnica-Worms for the *Cdc25a$^{fl/fl}$* mice, Dr. Greg Perry for flow cytometric assistance, Dr. Raymond Tennant for Tg.AC mice and Patrick Carroll for quantification of tumor area.

Conflict of Interest Statement: This research (LAH) was supported by funds from the National Institutes of Health and the State of Nebraska LB595. Carol Trempus is employed by the National Institutes of Health, which also supports her research.

References

1. Rogers,H.W. *et al.* (2010) Incidence estimate of nonmelanoma skin cancer in the United States, 2006. *Arch. Dermatol.*, **146**, 283–287.
2. Lo,H.L. *et al.* (2005) Differential biologic effects of CPD and 6-4PP UV-induced DNA damage on the induction of apoptosis and cell-cycle arrest. *BMC Cancer*, **5**, 135.
3. You,Y.H. *et al.* (2001) Cyclobutane pyrimidine dimers are responsible for the vast majority of mutations induced by UVB irradiation in mammalian cells. *J. Biol. Chem.*, **276**, 44688–44694.
4. Halliday,G.M. (2005) Inflammation, gene mutation and photoimmunosuppression in response to UVR-induced oxidative damage contributes to photocarcinogenesis. *Mutat. Res.*, **571**, 107–120.
5. Marrot,L. *et al.* (2008) Skin DNA photodamage and its biological consequences. *J. Am. Acad. Dermatol.*, **58**, S139–S148.
6. Shigenaga,M.K. *et al.* (1989) Urinary 8-hydroxy-2'-deoxyguanosine as a biological marker of in vivo oxidative DNA damage. *Proc. Natl. Acad. Sci. U.S.A.*, **86**, 9697–9701.
7. Ziech,D. *et al.* (2011) Reactive oxygen species (ROS)--induced genetic and epigenetic alterations in human carcinogenesis. *Mutat. Res.*, **711**, 167–173.
8. Boutros,R. *et al.* (2007) CDC25 phosphatases in cancer cells: key players? Good targets? *Nat. Rev. Cancer*, **7**, 495–507.

9. Sancar,A. *et al.* (2004) Molecular mechanisms of mammalian DNA repair and the DNA damage checkpoints. *Annu. Rev. Biochem.*, **73**, 39–85.
10. Zou,X. *et al.* (2001) The cell cycle-regulatory CDC25A phosphatase inhibits apoptosis signal-regulating kinase 1. *Mol. Cell Biol.*, **21**, 4818–4828.
11. Wang,Z. *et al.* (2008) Cdc25A protein phosphatase: a therapeutic target for liver cancer therapies. *Anticancer Agents Med. Chem.*, **8**, 863–871.
12. Lee,G. *et al.* (2009) Response of small intestinal epithelial cells to acute disruption of cell division through CDC25 deletion. *Proc. Natl. Acad. Sci. U.S.A.*, **106**, 4701–4706.
13. Vasioukhin,V. *et al.* (1999) The magical touch: genome targeting in epidermal stem cells induced by tamoxifen application to mouse skin. *Proc. Natl. Acad. Sci. U.S.A.*, **96**, 8551–8556.
14. Hansen,L.A. *et al.* (1998) Effect of the viable-yellow (Avy) agouti allele on skin tumorigenesis and humoral hypercalcemia in v-Ha-ras transgenci TG.AC mice. *Carcinogen*, **19**, 1837–1845.
15. Hansen,L.A. *et al.* (1990) Differential down-regulation of epidermal protein kinase C by 12-O-tetradecanoylphorbol-13-acetate and diacylglycerol: association with epidermal hyperplasia and tumor promotion. *Cancer Res.*, **50**, 5740–5745.
16. Madson,J.G. *et al.* (2009) Erbb2 suppresses DNA damage-induced checkpoint activation and UV-induced mouse skin tumorigenesis. *Am. J. Pathol.*, **174**, 2357–2366.
17. Vindelov,L.L. (1977) Flow microfluorometric analysis of nuclear DNA in cells from solid tumors and cell suspensions. A new method for rapid isolation and straining of nuclei. *Virchows Arch. B. Cell Pathol.*, **24**, 227–242.
18. Wulff,B.C. *et al.* (2008) Topical treatment with OGG1 enzyme affects UVB-induced skin carcinogenesis. *Photochem. Photobiol.*, **84**, 317–321.
19. Leisser,C. *et al.* (2004) Subcellular localisation of Cdc25A determines cell fate. *Cell Death Differ.,* **11**, 80–89.
20. Trempus,C.S. *et al.* (1998) Photocarcinogenesis and susceptibility to UV radiation in the *v-Ha-ras* transgenic Tg.AC mouse. *J. Invest. Dermatol*., **111**, 445–451.
21. Leder,A. *et al.* (1990) v-Ha-ras transgene abrogates the initiation step in mouse skin tumorigenesis: effects of phorbol esters and retinoic acid. *Proc. Natl. Acad. Sci. U.S.A*., **87**, 9178–9182.
22. van der Schroeff,J.G. *et al.* (1990) *Ras* oncogene mutations in basal cell carcinomas and squamous cell carcinomas of human skin. *J. Invest. Dermatol*., **94**, 423–425.
23. Pierceall,W.E. *et al.* (1991) *Ras* gene mutation and amplification in human nonmelanoma skin cancers. *Mol. Carcinog*., **4**, 196–202.
24. Ananthaswamy,H.N. *et al.* (1992) Molecular alterations in human skin tumors. *Prog. Clin. Biol. Res*., **376**, 61–84.
25. Pierceall,W.E. *et al.* (1992) N-ras mutation in ultraviolet radiation-induced murine skin cancers. *Cancer Res*., **52**, 3946–3951.
26. Dassule,H.R. *et al.* (2000) Sonic hedgehog regulates growth and morphogenesis of the tooth. *Development*, **127**, 4775–4785.
27. Lloyd,C. *et al.* (1995) The basal keratin network of stratified squamous epithelia: defining K15 function in the absence of K14. *J. Cell Biol*., **129**, 1329–1344.
28. Byrne,C. *et al.* (1994) Programming gene expression in developing epidermis. *Development*, **120**, 2369–2383.
29. Yu,B.D. *et al.* (2008) Skin and hair: models for exploring organ regeneration. *Hum. Mol. Genet*., **17**, R54–R59.
30. Nagy,A. (2000) Cre recombinase: the universal reagent for genome tailoring. *Genesis*, **26**, 99–109.
31. Pascucci,B. *et al.* (2011) Role of nucleotide excision repair proteins in oxidative DNA damage repair: an updating. *Biochemistry (Mosc.)*, **76**, 4–15.
32. Lynch,D. *et al.* (2007) Mouse skin models for carcinogenic hazard identification: utilities and challenges. *Tox. Pathol*., **35**, 853–864.
33. Kar,S. *et al.* (2003) Antitumor and anticarcinogenic actions of Cpd 5: a new class of protein phosphatase inhibitor. *Carcinogenesis*, **24**, 411–416.
34. Kar,S. *et al.* (2006) PM-20, a novel inhibitor of Cdc25A, induces extracellular signal-regulated kinase 1/2 phosphorylation and inhibits hepatocellular carcinoma growth in vitro and in vivo. *Mol. Cancer Ther*., **5**, 1511–1519.

Received November 22, 2011; revised March 29, 2012; accepted April 19, 2012